quantum reports

MDPI

Article

Schrödinger Equation with Geometric Constraints and Position-Dependent Mass: Linked Fractional Calculus Models

Ervin K. Lenzi [1,*], Luiz R. Evangelista [2,3], Haroldo V. Ribeiro [2] and Richard L. Magin [4]

[1] Departamento de Física, Universidade Estadual de Ponta Grossa, Ponta Grossa 84030-900, PR, Brazil
[2] Departamento de Física, Universidade Estadual de Maringá, Maringá 87020-900, PR, Brazil
[3] Dipartimento di Scienza Applicata del Politecnico di Torino, Corso Duca degli Abruzzi 24, 10129 Torino, Italy
[4] Department of Biomedical Engineering, University of Illinois at Chicago, Chicago, IL 60607, USA
* Correspondence: eklenzi@uepg.br; Tel.: +55-44-999-151257

Abstract: We investigate the solutions of a two-dimensional Schrödinger equation in the presence of geometric constraints, represented by a backbone structure with branches, by taking a position-dependent effective mass for each direction into account. We use Green's function approach to obtain the solutions, which are given in terms of stretched exponential functions. The results can be linked to the properties of the system and show anomalous spreading for the wave packet. We also analyze the interplay between the backbone structure with branches constraining the different directions and the effective mass. In particular, we show how a fractional Schrödinger equation emerges from this scenario.

Keywords: fractional dynamics; anomalous diffusion; comb-model

Citation: Lenzi, E.K.; Evangelista, L.R.; Ribeiro, H.V.; Magin, R.L. Schrödinger Equation with Geometric Constraints and Position-Dependent Mass: Linked Fractional Calculus Models. *Quantum Rep.* **2022**, *4*, 296–308. https://doi.org/10.3390/quantum4030021

Academic Editor: Lev Vaidman

Received: 20 June 2022
Accepted: 8 August 2022
Published: 14 August 2022

1. Introduction

The Schrödinger equation is of fundamental importance for describing phenomena occurring in the quantum world. Solutions to the Schrödinger equation are expressed in terms of the wave function $\Psi(x, y, t)$, whose modulus closely matches the experimental behavior of atoms and molecules. A crucial point in the quantum analysis concerns the probabilistic interpretation of $\Psi(x, y, t)$, which establishes a connection between with the Markovian or non-Markovian stochastic processes of the underlying molecular dynamics.

An example is the path integral formulation proposed by Richard Feynman [1], in which the ideas of stochastic motion connected with the Brownian motion are incorporated into the quantum-mechanical paths [1] (see, for instance, Refs. [2–6]). The path integral has been extended by incorporating the Lévy flights in the quantum-mechanical paths by Laskin [7–9], and this allowed us to obtain a fractional version of the Schrödinger equation, which is the primary focus of this paper.

The fractional Schrödinger equation generalizes the Schrödinger equation by incorporating fractional operators into the description of quantum phenomena [10–16]. However, there are other ways to account for the so-called, 'anomalous' quantum behavior predicted by the fractional wave functions of the fractional Schrödinger equation. One method is to assume the presence of a backbone structure with branches in the integer order quantum model [17–20] (see, for example, Figure 1), i.e., constraints between different directions along which the quantum dynamics are considered.

This structure imposes a condition on the spreading of the wave packet and, consequently, results in anomalous behavior for the variance, i.e., $\Delta x = \sqrt{\langle (x - \langle x \rangle)^2 \rangle} \propto t^{\delta}$ with $0 < \delta < 1$. Another way is to extend the classical Schrödinger equation by including a position-dependent effective mass [21–24]—a technique that has played an essential role in solid-state physics, such as semiconductors [25–27]. Hence, these cases allow us to consider other scenarios in addition to the standard cases [28] for the Schrödinger equation and, in particular, for mixing between them.

Our goal in this paper is to investigate the connection between geometrically constrained and effective mass integer-order models and the fractional two-dimensional Schrödinger equation. The cases considered for the Schrödinger equation are: (i) a backbone structure with branches and (ii) a spatial dependence mass for each direction. In this manner, we employ two different scenarios in a unified way and also connect them with the time-fractional Schrödinger equation. To do this, we start with the two-dimensional Schrödinger equation:

$$i\hbar\frac{\partial}{\partial t}\Psi(x,y,t) = -\hbar^2\delta\left(\frac{y}{l}\right)\frac{\partial}{\partial x}\left\{\frac{1}{m_x(x)}\frac{\partial}{\partial x}\Psi(x,y,t)\right\} - \hbar^2\frac{\partial}{\partial y}\left\{\frac{1}{m_y(y)}\frac{\partial}{\partial y}\Psi(x,y,t)\right\}. \quad (1)$$

The Dirac's delta present in Equation (1) is a consequence of the backbone structure with branches (see Figure 1) that constrain the wave function in the x- and y-directions. A similar situation was considered, for example, in Ref. [29] by analyzing the stochastic motion of particles in a two-dimensional space, i.e., along the x- and y-directions, for the motion of the particles by considering a constraint between these directions.

This approach has been connected to different situations, such as percolation clusters [30], anomalous diffusion on a comb structure [31], heterogeneous materials [32] and diffusion in random structures [33]. One of the main characteristics of the distributions related to these systems is the stretched exponential behavior, which is different from the Gaussian case and has implications for the shape and spreading of the wave packet.

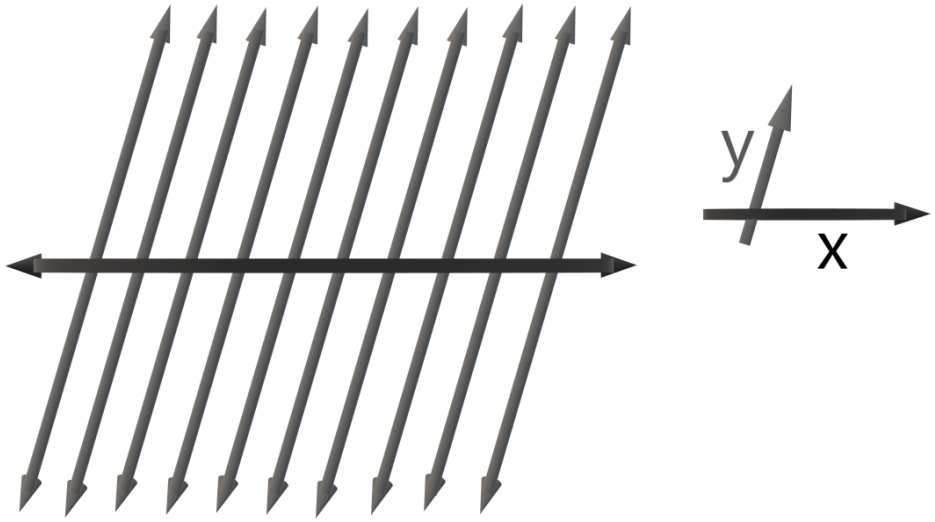

Figure 1. This figure illustrates the backbone structure connected with Equation (1).

Equation (1) considers an effective mass in the x- and y-directions in the forms $m_x(x) = 2m|x|^{\eta_x}$ and $m_y(y) = 2m|y|^{\eta_y}$, respectively. Before proceeding, we note that this spatial dependence has typically been employed in diffusion problems, such as diffusion on fractals [34,35], turbulence [36,37], diffusion and reaction on fractals [38] and solute transport in fractal porous media [39], where the properties of the media are responsible for anomalous diffusion.

Thus, the chosen mathematical expression of the effective mass is helpful to link our analysis to these transport problems or to others with similar structures or assumed wave-packet propagation. In addition, we remark that Equation (1) is characterized by an interplay between two different effects—namely, the constraints imposed by the structure along different directions and a position-dependent effective mass. In this framework, we investigate its solutions by using the Green's function approach and connect them with an anomalous spreading of the wave-packet. We also show that the properties of the media related to the spatial dependence on the mass can be connected with a time-fractional derivative.

The paper is organized as follows. In Section 2, the mathematical problem is formulated together with a discussion on the constraints. The results will be obtained by using analytical calculations. It is also possible to use numerical approaches as discussed in Refs. [40–44] to analyze Equation (1) by taking several conditions into account. The solutions are obtained, as described before, and the essential details of the calculations are exhibited. In Section 3, we discuss the main results of the analysis and present our concluding remarks.

2. Schrödinger's Equation and Geometric Constraints

Let us begin our analysis concerning Equation (1) by establishing the boundary and initial conditions to be satisfied by the solutions. They are: $\Psi(\pm\infty, y, t) = 0$, $\Psi(x, \pm\infty, t) = 0$ and $\Psi(x, y, 0) = \varphi(x, y)$. These boundary conditions are such that the system is free except for the geometric constraints imposed by the backbone structure. By using these conditions, we first tackle the case $\eta_x = 1$, with $\eta_y = 0$, and, after that, other cases are faced, for instance, $\eta_x = 0$, with $\eta_y \neq 0$ and $\eta_x \neq 0$, with $\eta_y \neq 0$.

2.1. $\eta_x \neq 0$ *and* $\eta_y = 0$

The Green's function for the first case, $\eta_x = 1$ with $\eta_y = 0$, related to Equation (1), can be obtained from the following equation:

$$i\hbar\frac{\partial}{\partial t}G(\mathbf{r},\mathbf{r}',t) + \frac{\hbar^2}{2m}\left\{\delta\left(\frac{y}{l}\right)\frac{\partial}{\partial x}\left[|x|^{-\eta_x}\frac{\partial}{\partial x}G(\mathbf{r},\mathbf{r}',t)\right] + \frac{\partial^2}{\partial y^2}G(\mathbf{r},\mathbf{r}',t)\right\} = i\hbar\delta(y-y')\delta(x-x')\delta(t)\,, \tag{2}$$

where $\mathbf{r} = (x, y)$. Equation (2) satisfies the conditions $G(\pm\infty, y, \mathbf{r}', t) = 0$, $G(x, \pm\infty, \mathbf{r}', t) = 0$ and $G(\mathbf{r}, \mathbf{r}', t) = 0$ for $t < 0$. The term related to the position-dependent effective mass allows us to connect the physical problem with the fractal derivatives [45], i.e., the differential operators:

$$\frac{\partial}{\partial m_{\mathcal{I},x}(x)}\Psi(x,y,t) = \lim_{x'\to x}\frac{\Psi(x,y,t)-\Psi(x',y,t)}{m_{\mathcal{I},x}(x)-m_{\mathcal{I},x}(x')} = \frac{1}{m_x(x)}\frac{\partial}{\partial x}\Psi(x,y,t)\,, \tag{3}$$

where $m_{\mathcal{I},x}(x) = \int^x d\bar{x} m_x(\bar{x})$ and, in this way, we can focus on the fractal aspects exhibited by the media. The substitution also has implications on the shape and on the spreading of the wave packet. In terms of the Green's function, the wave function $\Psi(\mathbf{r}, t)$ is given by

$$\Psi(\mathbf{r},t) = \int_{-\infty}^{\infty} dy' \int_{-\infty}^{\infty} dx' \varphi(\mathbf{r}')G(\mathbf{r},\mathbf{r}',t)\,, \tag{4}$$

which also allows us to analyze the influence of the effective mass on the solution. It is in this sense that we have the mentioned interplay between the backbone structure and effective mass, which is position-dependent with direct consequences on the spreading of the wave-packet. Equation (2) may be simplified by using the eigenfunctions of the Sturm-Liouville problem related to the following differential equation:

$$\frac{\partial}{\partial x}\left\{|x|^{-\eta_x}\frac{\partial}{\partial x}\psi_{\pm}(x,k_x)\right\} = -|k_x|^{2+\eta_x}\psi_{\pm}(x,k_x), \tag{5}$$

with

$$\psi_{+}(x,k_x) = (|k_x||x|)^{\frac{1}{2}(1+\eta_x)}\mathrm{J}_{-\nu_x}\left(2(|k_x||x|)^{\frac{1}{2}(2+\eta_x)}/(2+\eta_x)\right) \quad \text{and} \tag{6}$$

$$\psi_{-}(x,k_x) = xk_x(|k_x||x|)^{\frac{1}{2}(1+\eta_x)-1}\mathrm{J}_{\nu_x}\left(2(|k_x||x|)^{\frac{1}{2}(2+\eta_x)}/(2+\eta_x)\right)\,, \tag{7}$$

where the sub-indexes $+$ and $-$ refer to the odd and even solutions, $\nu_x = (1+\eta_x)/(2+\eta_x)$, and $\mathrm{J}_{\nu_x}(x)$ is the Bessel function [46]. By using the eigenfunctions defined by Equations (6)

and (7), it is possible to obtain the Green's function and, consequently, the solution to the problem. Here, we follow the procedure employed in Refs. [47–49] to work out the problems with this type of spatial dependence on the mass for the x- and y-directions. To do this, we consider the Green's function given by:

$$G(\mathbf{r},\mathbf{r}',t) = \frac{1}{2}\int_{-\infty}^{\infty} dk_x \Big[\psi_+(x,k_x)\tilde{G}_+(k_x,y,\mathbf{r}',t) + \psi_-(x,k_x)\tilde{G}_-(k_x,y,\mathbf{r}',t)\Big], \tag{8}$$

with

$$\tilde{G}_\pm(k_x,y,\mathbf{r}',t) = \frac{1}{2}\int_{-\infty}^{\infty} dx \psi_\pm(x,k_x)G(\mathbf{r},\mathbf{r}',t), \tag{9}$$

where $G_\pm(k_x,y,\mathbf{r}',t)$ is determined by Equation (2). By substituting Equation (8) into Equation (2) and exploring the orthogonality of the eigenfunctions and the Fourier transform in the y-variable, i.e., ($\mathcal{F}_y\{G(\mathbf{r},\mathbf{r}',t);k_y\} = \bar{G}(x,k_y,\mathbf{r}',t)$ and $\mathcal{F}_y^{-1}\{\bar{G}(x,k_y,\mathbf{r}',t;y)\} = G(\mathbf{r},\mathbf{r}',t)$), we have

$$\begin{aligned} i\hbar\frac{\partial}{\partial t}\tilde{\bar{G}}_\pm(k_x,k_y,\mathbf{r}',t) &- \frac{\hbar^2 l}{2m}|k_x|^{2+\eta_x}\tilde{G}_\pm(k_x,0,\mathbf{r}',t) \\ &- \frac{\hbar^2 k_y^2}{2m}\tilde{\bar{G}}_\pm(k_x,k_y,\mathbf{r}',t) = \frac{1}{2}i\hbar\psi_\pm(x',k_x)e^{-ik_y y'}\delta(t)\,. \end{aligned} \tag{10}$$

Equation (10) may be written as

$$\begin{aligned} \tilde{\bar{G}}_\pm(k_x,y,\mathbf{r}',t) &= \frac{1}{2}\psi_\pm(x',k_x)G_y(y-y',t) \\ &- \frac{i\hbar l}{2m}|k_x|^{2+\eta_x}\int_0^t dt' G_y(y,t-t')\tilde{\bar{G}}_\pm(k_x,0,\mathbf{r}',t'), \end{aligned} \tag{11}$$

where

$$G_y(y,t) = \sqrt{\frac{m}{2\pi i\hbar t}}e^{-\frac{m}{2i\hbar t}y^2} \tag{12}$$

is the standard free particle propagator in the y-direction. From these equations, the Green's function on the backbone structure in the Laplace domain ($\mathcal{L}\{G(\mathbf{r},\mathbf{r}',t);s\} = \widehat{G}(\mathbf{r},\mathbf{r}',s)$ and $\mathcal{L}^{-1}\{\widehat{G}(\mathbf{r},\mathbf{r}',s);t\} = G(\mathbf{r},\mathbf{r}',t)$) is given by

$$\widehat{\tilde{G}}_\pm(k_x,0,\mathbf{r}',s) = \frac{1}{2}\frac{\psi_\pm(x',k_x)}{1+\frac{l}{2}\sqrt{\frac{i\hbar}{2ms}}|k_x|^{2+\eta_x}}\widehat{G}_y(y',s). \tag{13}$$

The substitution of Equation (13) into Equation (11) yields

$$\begin{aligned} \widehat{G}(\mathbf{r},\mathbf{r}',s) &= \delta(x-x')\left[\widehat{G}_y(y-y',s) - \widehat{G}_y(|y|+|y'|,s)\right] \\ &+ \frac{1}{2}\int_0^\infty dk_x \frac{\widehat{G}_y(|y|+|y'|,s)}{1+\frac{l}{2}\sqrt{\frac{i\hbar}{2ms}}k_x^{2+\eta_x}}\sum_{n=-,+}\psi_n(x,k_x)\psi_n(x',k_x). \end{aligned} \tag{14}$$

Using the inverse Laplace transform of Equation (14), the Green's function is given by

$$\begin{aligned} G(\mathbf{r},\mathbf{r}',t) &= \delta(x-x')\left[G_y(y-y',t) - G_y(|y|+|y'|,t)\right] \\ &+ \frac{1}{\sqrt{\pi}}\left(\frac{m}{2i\hbar t}\right)^{\frac{3}{2}}\int_0^\infty du\Big[|y|+|y'|+u\Big]e^{-\frac{m}{2i\hbar t}(|y|+|y'|+u)^2}\Phi_{\nu_x}(x,x',u), \end{aligned} \tag{15}$$

with

$$\Phi_{\nu_x}(x,x',u)=\frac{2+\eta_x}{\alpha_x u}\left(|x'||x|\right)^{\frac{1}{2}(1+\eta_x)}\exp\left[-\frac{1}{\alpha_x u}\left(|x|^{2+\eta_x}+|x'|^{2+\eta_x}\right)\right]$$
$$\times\left\{I_{-\nu_x}\left[\left(2|x'||x|\right)^{\frac{1}{2}(2+\eta_x)}/(\alpha_x u)\right]+\frac{xx'}{|x||x'|}I_{\nu_x}\left[\left(2|x'||x|\right)^{\frac{1}{2}(2+\eta_x)}/(\alpha_x u)\right]\right\}, \quad (16)$$

where $\alpha_x = (2+\eta_x)^2(l/2)$, and $I_{\nu_x}(x)$ corresponds to the Bessel function of modified argument [46]. Figures 2 and 3 exhibit a two-dimensional profile of the wave function for $\eta_x = 1/2$ and $\eta_x = -1/2$. These values of the exponents are responsible for the different shapes of the wave function.

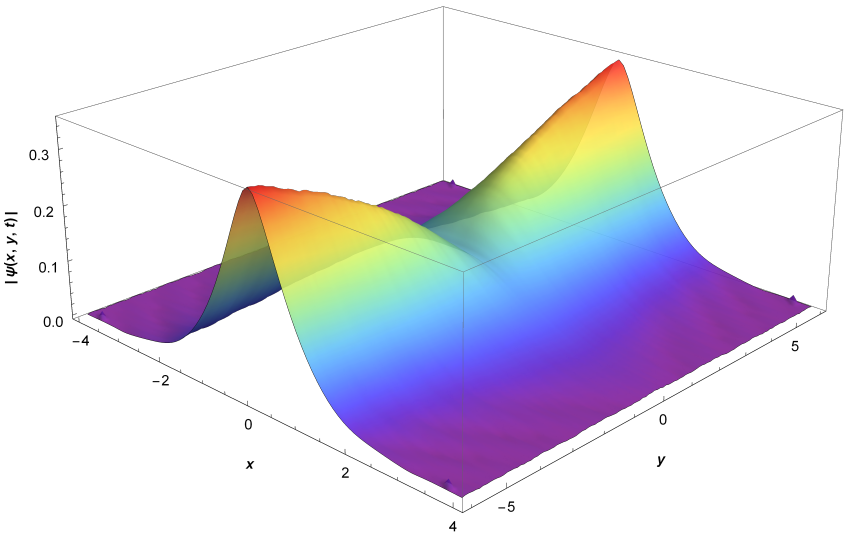

Figure 2. Profile of $|\Psi(x,y,t)|$ for $\eta_x = 1/2$. For illustrative purposes, we consider $\hbar t/(2m) = 1$, $l = 1$ and the initial condition $\varphi(x) = \delta(x)\delta(y)$.

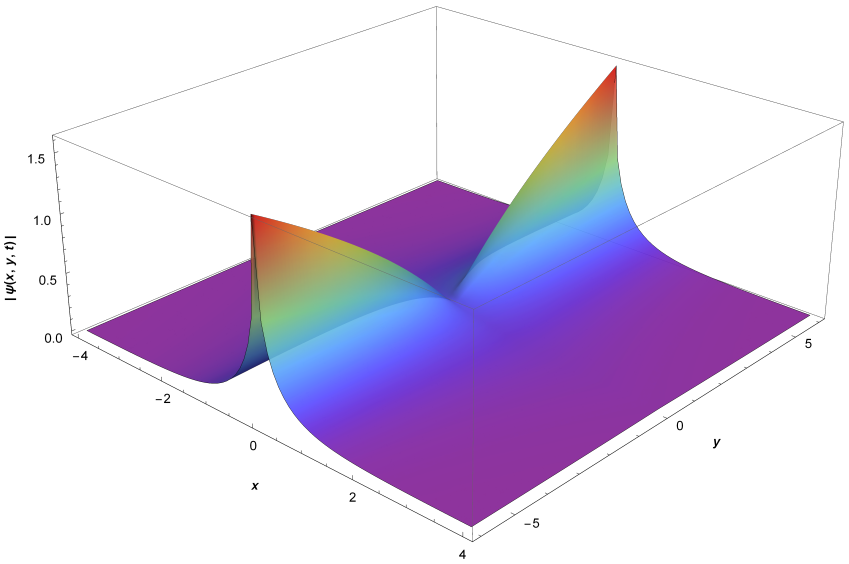

Figure 3. Profile of $|\Psi(x,y,t)|$ for $\eta_x = -1/2$. The other parameters are the same as in Figure 2.

2.2. $\eta_x = 0$ *and* $\eta_y \neq 0$

Let us consider the case $\eta_x = 0$ and $\eta_y \neq 0$. This way, the equation for the Green's function is

$$i\hbar\frac{\partial}{\partial t}G(\mathbf{r},\mathbf{r}',t) + \frac{\hbar^2}{2m}\left\{\delta\left(\frac{y}{l}\right)\frac{\partial^2}{\partial x^2}G(\mathbf{r},\mathbf{r}',t) + \frac{\partial}{\partial y}\left[|y|^{-\eta_y}\frac{\partial}{\partial y}G(\mathbf{r},\mathbf{r}',t)\right]\right\} = i\hbar\delta(y-y')\delta(x-x')\delta(t). \quad (17)$$

The solutions of Equation (17) also satisfy the conditions $G(\pm\infty, y, \mathbf{r}', t) = 0$, $G(x, \pm\infty, \mathbf{r}', t) = 0$ and $G(\mathbf{r}, \mathbf{r}', t) = 0$ for $t < 0$. In Equation (17), the term related to the variable y can also be related to the fractal derivatives [45], as in the case of Equation (2).

The wave function $\Psi(\mathbf{r}, t)$ may be expressed as in the preceding case, i.e., by Equation (4). A similar procedure yields the Green's function by using the integral transform in the y-variable as follows:

$$G(\mathbf{r},\mathbf{r}',t) = \frac{1}{2}\int_{-\infty}^{\infty} dk_y\left[\psi_+(y,k_y)\widetilde{G}_{+,y}(x,k_y,\mathbf{r}',t) + \psi_-(y,k_y)\widetilde{G}_{-,y}(x,k_y,\mathbf{r}',t)\right], \quad (18)$$

with

$$\widetilde{G}_{\pm,y}(x,k_y,\mathbf{r}',t) = \frac{1}{2}\int_{-\infty}^{\infty} dy\psi_\pm(y,k_y)G(\mathbf{r},\mathbf{r}',t), \quad (19)$$

where $G_\pm(x,k_y,\mathbf{r}',t)$ is determined by Equation (17). The functions $\psi_\pm$ used in this case are the same as the ones used in the preceding case with $(x,k_x) \to (y,k_y)$, $\eta_x \to \eta_y$ and $\nu_x \to \nu_y$. By substituting Equation (18) in Equation (17) and using the orthogonality of the eigenfunctions with the Fourier transform in the y-variable, we obtain

$$i\hbar\frac{\partial}{\partial t}\widetilde{G}_{\pm,y}(k_x,k_y,\mathbf{r}',t) - \frac{\hbar^2 l}{2m}|k_x|^2\psi_\pm(0,k_y)\bar{G}(k_x,0,\mathbf{r}',t) - \frac{\hbar^2}{2m}|k_y|^{2+\eta_y}\tilde{G}_{\pm,y}(k_x,k_y,\mathbf{r}',t) = \frac{1}{2}i\hbar\psi_\pm(y',k_y)e^{-ik_x x'}\delta(t). \quad (20)$$

Before proceeding, we notice that differently from Equation (10), we have now the presence of $\psi_\pm(0,k_y)$ in the term related to the backbone structure. This feature shows that the system may be trapped in the branches depending on the initial condition. Equation (20) may also be written as an integral equation—namely,

$$\widetilde{\bar{G}}_{\pm,y}(k_x,k_y,\mathbf{r}',t) = \widetilde{G}_{\nu_y,\pm}(k_y,y',t)e^{-ik_x x'} - \frac{i\hbar l}{2m}|k_x|^2\int_0^t dt'\widetilde{G}_{\nu_y,\pm}(k_y,0,t-t')\bar{G}(k_x,0,\mathbf{r}',t'), \quad (21)$$

where

$$\widehat{\widetilde{G}}_{\nu_y,\pm}(k_y,y',s) = \frac{1}{2}\frac{\psi_\pm(y',k_y)}{s+\frac{i\hbar}{2m}|k_y|^{2+\eta_y}} \quad (22)$$

is the free particle propagator in the y-direction related to the odd and even eigenfunctions in the Laplace space. After obtaining the inverse integral transforms, we have

$$G_{\nu_y,\pm}(y,y',t) = \frac{m}{(2+\eta_y)i\hbar t}e^{-\frac{2m}{(2+\eta_y)^2 i\hbar t}\left(|y|^{2+\eta_y}+|y'|^{2+\eta_y}\right)} \times \begin{cases} (|y||y'|)^{\frac{1}{2}(1+\eta_y)}I_{-\nu_y}\left(\frac{4m}{(2+\eta_y)^2 i\hbar t}(|y||y'|)^{\frac{1}{2}(2+\eta_y)}\right) \\ yy'(|y||y'|)^{\frac{1}{2}(1+\eta_y)-1}I_{\nu_y}\left(\frac{4m}{(2+\eta_y)^2 i\hbar t}(|y||y'|)^{\frac{1}{2}(2+\eta_y)}\right) \end{cases}. \quad (23)$$

In the Laplace domains, the Green's function in the backbone structure for this case is

$$\widehat{\bar{G}}(k_x, 0, \mathbf{r}', s) = \frac{e^{-ik_x x'}}{1 + \frac{i\hbar l}{2m}|k_x|^2 \widehat{G}_{\nu_y,+}(0,0,s)} \widehat{G}_{\nu_y,+}(0, y', s), \tag{24}$$

where

$$G_{\nu_y,+}(0, y', t) = \frac{2+\eta_y}{2\Gamma\left(\frac{1}{2+\eta_y}\right)} \left(\frac{2m}{(2+\eta_y)^2 i\hbar t}\right)^{\frac{1}{2+\eta_y}} e^{-\frac{2m|y'|^{2+\eta_y}}{(2+\eta_y)^2 i\hbar t}}. \tag{25}$$

The substitution of Equation (24) into Equation (21), in the Laplace domain, yields

$$\begin{aligned} \widehat{G}(\mathbf{r}, \mathbf{r}', s) &= \delta(x - x') \Bigg\{ \left[\widehat{G}_{\nu_y,+}(y, y', s) - \frac{s^{\eta'_y}}{\widehat{G}_{\nu_y,+}(0,0,1)} \widehat{G}_{\nu_y,+}(y, 0, s) \widehat{G}_{\nu_y,+}(0, y', s) \right] \\ &+ \widehat{G}_{\nu_y,-}(y, y', s) \Bigg\} \\ &+ \frac{1}{\widehat{G}_{\nu_y,+}(0,0,s)} \int_{-\infty}^{\infty} \frac{dk_x}{2\pi} \frac{e^{ik_x(x-x')}}{1 + \frac{i\hbar l}{2m}|k_x|^2 \widehat{G}_{\nu_y,+}(0,0,s)} \widehat{G}_{\nu_y,+}(y, 0, s) \widehat{G}_{\nu_y,+}(0, y', s), \end{aligned} \tag{26}$$

with $\eta'_y = 1 - 1/(2+\eta_y)$. After obtaining the inverse Laplace transform of Equation (26), the Green's function may be written as

$$\begin{aligned} G(\mathbf{r}, \mathbf{r}', t) &= \delta(x - x') \Bigg\{ \left[G_{\nu_y,+}(y, y', t) - \mathcal{D}_t^{\eta'_y} \left(\int_0^t \frac{dt'}{\alpha_y} G_{\nu_y,+}(y, 0, t') G_{\nu_y,+}(0, y', t - t') \right) \right] \\ &+ G_{\nu_y,-}(y, y', t) \Bigg\} \\ &+ \frac{1}{|x|} \int_0^t dt' t'^{\eta'_y - 1} \, \mathrm{H}_{1,1}^{1,0} \left[\frac{2m|x|^2}{i\hbar l \alpha_y t'^{\eta'_y}} \middle| \begin{matrix} (\eta'_y, \eta'_y) \\ (1,2) \end{matrix} \right] \Lambda_y(y, y', t - t'), \end{aligned} \tag{27}$$

for $0 < \eta'_y < 1$ with

$$\Lambda_y(y, y', t) = \frac{1}{\alpha_y} \int_0^t dt' \left(\mathcal{D}_{t'}^{\eta'_y} G_{\nu_y,+}(y, 0, t') \right) \left(\mathcal{D}_{t''}^{\eta'_y} G_{\nu_y,+}(y, 0, t'') \Big|_{t''=t-t'} \right), \tag{28}$$

in which $\alpha_y = \widehat{G}_{\nu_y,+}(0,0,1)$ and the operator $\mathcal{D}_t^{\eta'_y}(\cdots)$ is the Riemann–Liouville fractional operator [10] of order η'_y, defined by

$$\mathcal{D}_t^{\eta'_y} G_{\nu_y,+}(y, y', t) = \frac{1}{\Gamma\left(\eta'_y\right)} \frac{\partial}{\partial t} \int_0^t dt' \frac{1}{(t - t')^{1-\eta'_y}} G_{\nu_y,+}(y, y', t'). \tag{29}$$

In Equation (27), we have the Fox H function, usually represented [10] by

$$\mathrm{H}_{p,q}^{m,n}\left[z \middle| \begin{matrix} (a_p, A_p) \\ (b_q, B_q) \end{matrix} \right] = \mathrm{H}_{p,q}^{m,n}\left[z \middle| \begin{matrix} (a_1, A_1) \cdots (a_p, A_p) \\ (b_1, B_1) \cdots (b_q, B_q) \end{matrix} \right] = \frac{1}{2\pi i} \int_L ds \chi(s) z^s \tag{30}$$

$$\chi(s) = \frac{\prod_{j=1}^{m} \Gamma\left(b_j - B_j s\right) \prod_{j=1}^{n} \Gamma\left(1 - a_j + A_j s\right)}{\prod_{j=1}^{q} \Gamma\left(1 - b_j + B_j s\right) \prod_{j=1}^{p} \Gamma\left(a_j - A_j s\right)}, \tag{31}$$

which involves Mellin–Barnes integrals [10].

Figure 4 exhibits some trends of $\Psi(x, y, t)$ in particular cases for different values of η_y. Figure 4a,b show that heterogeneity in the y-direction, i.e., $\eta'_y \neq 1$, has a clear effect on the propagation of the wave function in the x-direction, promoting a different behavior of $\eta'_y \neq 1$. Figures 4c,d show the spatial profile in the y-direction for different values of η'_y.

We notice that the value $\eta_y' = -1/2$ is responsible for an amplitude that is greater than the amplitude corresponding to the other values.

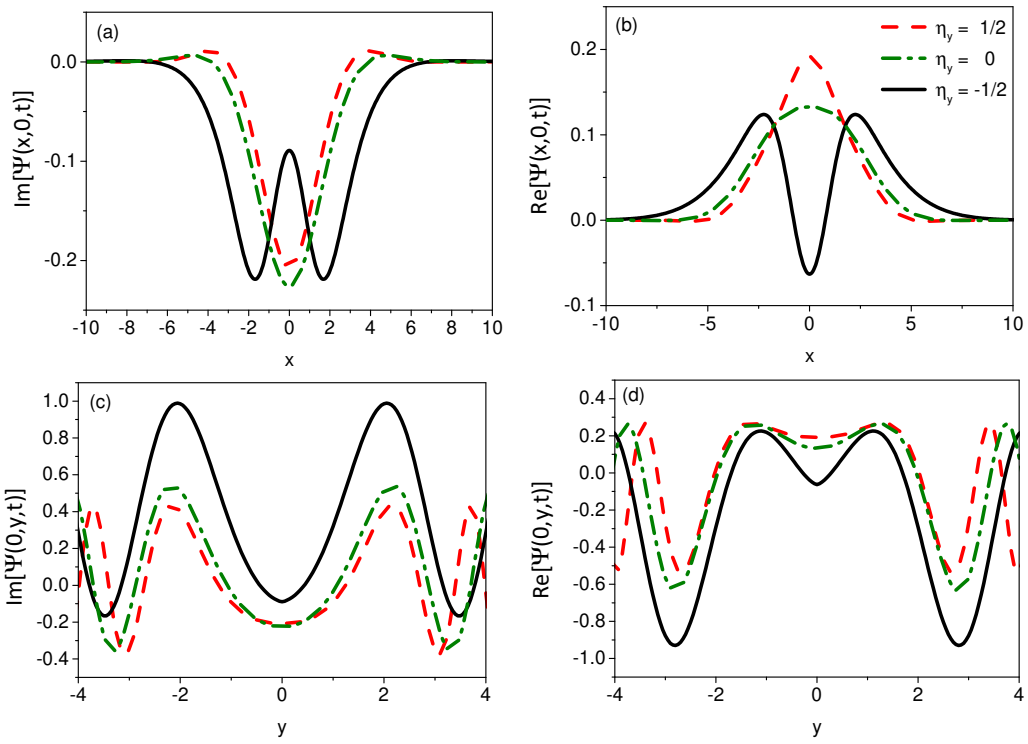

Figure 4. (**a**) Imaginary and (**b**) Real parts of $\Psi(x,0,t)$ vs. x for $\eta_y' = -1/2$, 0 and $1/2$. (**c**) Imaginary and (**d**) Real parts of $\Psi(0,y,t)$ vs. y for the same values of the parameters. The curves are depicted for $\hbar t/m = 1$, $l/t^{\eta_y'} = 1$, and the initial condition $\varphi(x,y) = \delta(y)e^{-x^2/(2\sigma^2)}/(\sqrt{\pi\sigma^2})$, with $\sigma^2 = 1$.

From the Green's function results, we observe that the presence of an effective mass depending on the y-direction, i.e., on the branches, promotes an anomalous spreading of the wave-packet in time, depending on the values of η_y'. This may be related to a time-fractional derivative and, for this reason, we may reduce Equation (26) to a one-dimensional equation involving only the x-variable to evidence this feature. By some suitable simplifications, after taking $y' = 0$ and performing integration in the y-variable, we obtain

$$\widehat{\bar{G}}_r(k_x, x', s) \quad = \quad E_{\eta_y'}\left(-\frac{i\hbar l}{2m}\alpha_y |k_x|^2 t^{\eta_y'}\right) e^{-ik_x x'}, \tag{32}$$

where $E_{\eta_y'}(t)$ is the Mittag–Leffler function [10] and $\widehat{\bar{G}}_r(k_x, x', s) = \int_{-\infty}^{\infty} \widehat{\bar{G}}(k_x, y, x', 0, s)dy$.

The Mittag–Leffler function is defined as:

$$E_\alpha(x) = \sum_{n=0}^{\infty} \frac{x^n}{\Gamma(1+\alpha n)}\,, \tag{33}$$

and this recovers the exponential form when $\alpha = 1$. The behavior of the Mittag–Leffler function for $x \to -\infty$ is $E_\alpha(x) \sim -1/[\Gamma(1-\alpha)x]$, i.e., a power–law behavior in the asymptotic limit. This feature demonstrates that Equation (32) has an unconventional relaxation process directly connected with the spatial dependence on the mass and on the geometric constraints of the system. These calculations suppose the following equation determining the Green's function

$$i\hbar \frac{\partial^{\eta_y'}}{\partial t^{\eta_y'}} G_r(x, x', t) + l\frac{\hbar^2}{2m}\alpha_y \frac{\partial^2}{\partial x^2} G_r(x, x', t) = i\hbar\delta(x - x')\delta(t), \tag{34}$$

whose solution is

$$G_r(x,x',t) = \frac{1}{|x-x'|}\, \mathrm{H}^{1,0}_{1,1}\left[\frac{2m|x-x'|^2}{i\hbar l \alpha_y t^{\eta'_y}} \middle| \begin{matrix} (\eta'_y, \eta'_y) \\ (1,2) \end{matrix} \right], \tag{35}$$

which is the inverse Fourier transform of Equation (32). In Figure 5,

$$\Psi_x(x,t) = \int_{-\infty}^{\infty} dx' \varphi_x(x) G_r(x,x',t) \tag{36}$$

is exhibited versus x for different values of the parameter η'_y. We notice that the values of $\eta_y \neq 0$ change the solutions in the x-direction, which present a stretched exponential trend.

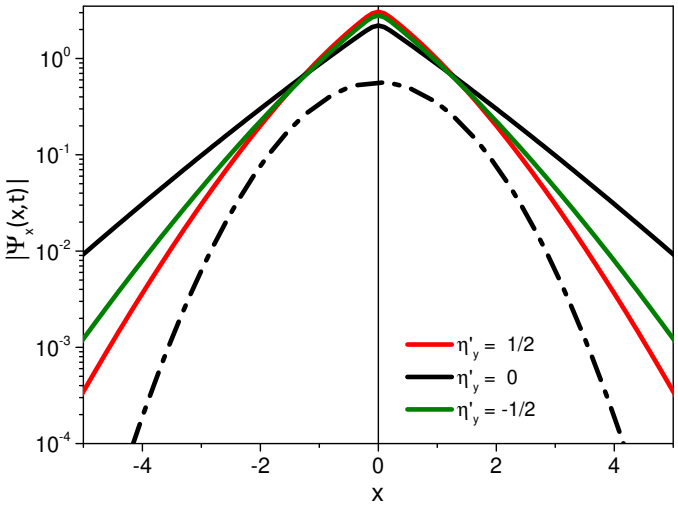

Figure 5. $|\Psi_x(x,t)|$ vs. x, for different values of η'_y. The dashed-dotted line corresponds to the wave function $\Psi_x(x) = e^{x^2/2}/\sqrt{\pi}$, which was incorporated for comparative purposes to evidence the effect of $\eta'_y \neq 1$ on the solutions of the Schrödinger equation. The curves are drawn for $\hbar l t^{\eta'_y}/(2m) = 1$, $l = 1$ and the initial condition $\varphi_x(x) = e^{-x^2/(2\sigma^2)}/(\sqrt{\pi\sigma^2})$, with $\sigma^2 = 0.01$.

Figure 6 shows the behavior of $1/|\Psi_x(0,t)|^2$, which is connected with $(\Delta x)^2$ through the relation $\Delta x \sim 1/|\Psi_x(0,t)|^2$. It shows the effect of the index η_y on the x-direction and, in particular, on the spreading of the wave packet, which exhibits an anomalous behavior, i.e., different from the behavior $\Delta x \sim t$ verified for the standard case in the limit of long times.

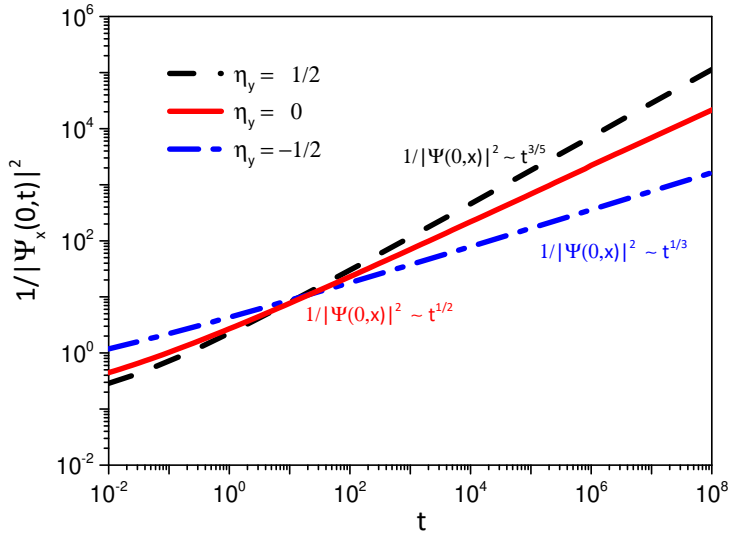

Figure 6. This figure illustrates the behavior of $1/|\Psi_x(0,t)|^2$ for different values of η_y. We consider, for simplicity, $\hbar l/(2m) = 1$, $l = 1$ and the initial condition $\varphi_x(x) = e^{-x^2/(2\sigma^2)}/(\sqrt{\pi\sigma^2})$, with $\sigma^2 = 0.01$.

2.3. $\eta_x \neq 0$ and $\eta_y \neq 0$

Finally, let us consider the more general case in which $\eta_x \neq 0$ and $\eta_y \neq 0$. For this case, the Green's function is now obtained from the equation:

$$\begin{aligned} i\hbar\frac{\partial}{\partial t}G(\mathbf{r},\mathbf{r}',t) \; + \; \delta\Big(\frac{y}{l}\Big)\frac{\hbar^2}{2m}\frac{\partial}{\partial x}\Big[|x|^{\eta_x}\frac{\partial}{\partial x}G(\mathbf{r},\mathbf{r}',t)\Big] + \frac{\hbar^2}{2m}\frac{\partial}{\partial y}\Big[|y|^{-\eta_y}\frac{\partial}{\partial y}G(\mathbf{r},\mathbf{r}',t)\Big] \\ = \; i\hbar\delta(y-y')\delta(x-x')\delta(t). \end{aligned} \tag{37}$$

By operating in a way similar to the methods employed in the preceding sections and noticing that Equation (37) is also subjected to the same conditions as before, the Green's function may be obtained as

$$G(\mathbf{r},\mathbf{r}',t) \; = \; \frac{1}{4}\int_{-\infty}^{\infty}dk_x\int_{-\infty}^{\infty}dk_y\sum_{\beta,\gamma=+,-}\psi_\beta(x,k_x)\psi_\gamma(y,k_y)\widetilde{G}_{\beta,\gamma,xy}(k_x,k_y,\mathbf{r}',t) \tag{38}$$

with

$$\widetilde{G}_{\beta,\gamma,xy}(k_x,k_y\mathbf{r}',t) = \frac{1}{4}\int_{-\infty}^{\infty}dx\int_{-\infty}^{\infty}dy\psi_\beta(x,k_x)\psi_\gamma(y,k_y)G(\mathbf{r},\mathbf{r}',t), \tag{39}$$

where $G_{\beta,\gamma,xy}(k_x,k_y,\mathbf{r}',t)$ is determined by Equation (37), and the indexes β and γ reflect the sums over the eigenfunctions odd $-$ and even $+$. By substituting Equation (38) in Equation (37) and using the orthogonality of the eigenfunctions, we obtain

$$\begin{aligned} i\hbar\frac{\partial}{\partial t}\widetilde{G}_{\beta,\gamma,xy}(k_x,k_y,\mathbf{r}',t) \; - \; \frac{\hbar^2 l}{2m}|k_x|^{2+\eta_x}\psi_\gamma(0,k_y)\widetilde{G}_{\beta,x}(k_x,0,\mathbf{r}',t) \\ - \; \frac{\hbar^2}{2m}|k_y|^{2+\eta_y}\widetilde{G}_{\beta,\gamma,xy}(k_x,k_y,\mathbf{r}',t) = \frac{i\hbar}{4}\psi_\gamma(y',k_y)\psi_\beta(x',k_x)\delta(t). \end{aligned} \tag{40}$$

The integral equation related to Equation (40) is

$$\begin{aligned} \widetilde{G}_{\beta,\gamma,xy}(k_x,k_y,\mathbf{r}',t) \; &= \; \psi_\beta(x',k_x)\widetilde{G}_{\nu_y,\gamma}(k_y,y',t) \\ &- \; \frac{i\hbar l}{2m}|k_x|^{2+\eta_x}\int_0^t dt'\widetilde{G}_{\nu_y,\gamma}(k_y,0,t-t')\widetilde{G}_{\beta,x}(k_x,0,\mathbf{r}',t'), \end{aligned} \tag{41}$$

where

$$\widehat{\widetilde{G}}_{\nu_y,\gamma}(k_y,y',s) = \frac{1}{2}\frac{\psi_\gamma(y',k_y)}{s+\frac{i\hbar}{2m}|k_y|^{2+\eta_y}} \tag{42}$$

is the free particle propagator in the y-direction in the Laplace domain. By using these results, we can show that, in the Laplace domain, the Green's function on the backbone structure is

$$\widehat{\widetilde{G}}_{\beta,x}(k_x,0,\mathbf{r}',s) = \frac{\psi_\beta(x',k_x)}{1+\frac{i\hbar l}{2m}|k_x|^{2+\eta_x}\widehat{G}_{\nu_y,+}(0,0,s)}\widehat{G}_{\nu_y,+}(0,y',s). \tag{43}$$

The substitution of Equation (24) into Equation (41) yields, in the Laplace domain:

$$\begin{aligned} \widehat{G}(\mathbf{r},\mathbf{r}',s) \; &= \; \delta(x-x')\Bigg\{\Big[\widehat{G}_{\nu_y,+}(y,y',s) - \frac{s^{\eta_y'}}{\alpha_y}\widehat{G}_{\nu_y,+}(y,0,s)\widehat{G}_{\nu_y,+}(0,y',s)\Big] \\ &+ \; \widehat{G}_{\nu_y,-}(y,y',s)\Bigg\} \\ &+ \; \int_{-\infty}^{\infty}dk_x\frac{s^{\eta_y'}\widehat{G}_{\nu_y,+}(y,0,s)\widehat{G}_{\nu_y,+}(0,y',s)}{2\alpha_y\Big(1+\frac{i\hbar l}{2m}|k_x|^{2+\eta_x}\widehat{G}_{\nu_y,+}(0,0,s)\Big)}\sum_{\beta=-,+}\psi_\beta(x,k_x)\psi_\beta(x',k_x). \end{aligned} \tag{44}$$

After obtaining the inverse Laplace transform of Equation (14), the Green's function is finally written as

$$\begin{aligned} G(\mathbf{r},\mathbf{r}',t) &= \delta(x-x')\Bigg\{\left[G_{\nu_y,+}(y,y',t) - \mathcal{D}_t^{\eta_y'}\left(\int_0^t \frac{dt'}{\alpha_y} G_{\nu_y,+}(y,0,t') G_{\nu_y,+}(0,y',t-t')\right)\right] \\ &+ G_{\nu_y,-}(y,y',t)\Bigg\} \\ &+ \int_0^\infty du \Phi_{\nu_x}\left(x,x',\alpha_y' u\right) \int_0^t \frac{dt'}{t'}\, \mathrm{H}_{1,1}^{1,0}\left[\frac{u}{t'^{\eta_y'}}\middle| \begin{matrix}(0,\eta_y')\\(0,1)\end{matrix}\right] \Lambda_y(y,y',t-t'), \end{aligned} \tag{45}$$

where $\alpha_y' = i\hbar\alpha_y/m$. Again, we notice that similarly to the result obtained in the previous cases, the heterogeneity present in the y-direction combined with the backbone structure introduces into Equation (45) the time-fractional derivatives of order η_y'. Furthermore, Equation (45) promotes an anomalous spreading of the wave-packet in view of the unusual relaxation processes resulting from the combination of the effective mass with the constrained structure of the comb-model.

3. Discussion and Conclusions

We analyzed the free-particle Schrödinger equation subjected to a backbone structure with branches, which constrains the x- and y-directions as well as the position-dependent effective mass for the x-direction and the y-direction. In this scenario, we first considered a position-dependent effective mass in the x-direction. This case exhibited solutions different from the usual ones, i.e., they were not given in terms of Gaussians. The second case analyzed the presence of a position-dependent effective mass in the y-direction by taking the backbone structure with branches into account. This case allowed us to connect the Green's function of the problem with a time-fractional Schrödinger equation with $0 < \eta_y' < 1$.

This feature is interesting since we are connecting a fractional time derivative with the combined backbone structure and an effective mass model, i.e., two different effects combine to yield a form equivalent to a fractional differential equation. For this case, we showed that the wave package has an anomalous spreading due to the backbone structure and the position-dependent mass.

The third case was handled with a position-dependent effective mass for the x- and the y-directions. The solutions were given in terms of a stretched exponential behavior for this general situation, which is expected to be connected to non-Markovian processes. This new feature is directly related to the characteristics of the medium—here represented by the backbone structure combined with the presence of an effective mass dependent on the position. In addition, we discussed the idea that the heterogeneity of the system promoted by the comb-model and the effective mass model can be related to a fractional Schrödinger equation for the x-direction. The whole formalism, presented in steps of increasing complexity, paves the way for future work on the influence of the spreading of wave packets in constrained quantum systems.

Author Contributions: Conceptualization, E.K.L., L.R.E., H.V.R. and R.L.M.; methodology, E.K.L., L.R.E., H.V.R. and R.L.M.; formal analysis, E.K.L., L.R.E., H.V.R. and R.L.M.; investigation, E.K.L., L.R.E., H.V.R. and R.L.M.; writing—original draft preparation, E.K.L., L.R.E., H.V.R. and R.L.M.; writing—review and editing, E.K.L., L.R.E., H.V.R. and R.L.M. All authors have read and agreed to the published version of the manuscript.

Funding: E.K.L. thanks the partial financial support of the CNPq under Grant No. 302983/2018-0.

Institutional Review Board Statement: Not applicable.

Informed Consent Statement: Not applicable.

Data Availability Statement: The authors declare that the data supporting the findings of this study are available within the article.

Acknowledgments: L.R.E. was partially supported by the Program of Visiting Professors of Politecnico di Torino (Italy).

Conflicts of Interest: The authors declare no conflict of interest.

References

1. Feynman, R.P.; Hibbs, A.R.; Styer, D.F. *Quantum Mechanics and Path Integrals*; Courier Corporation: Chelmsford, MA, USA, 2010.
2. Nelson, E. Derivation of the Schrödinger equation from Newtonian mechanics. *Phys. Rev.* **1966**, *150*, 1079. [CrossRef]
3. Nelson, E. *Dynamical Theories of Brownian Motion*; Princeton University Press: Princeton, NJ, USA, 2020; Volume 106.
4. Wallstrom, T.C. On the derivation of the Schrödinger equation from stochastic mechanics. *Found. Phys. Lett.* **1989**, *2*, 113–126. [CrossRef]
5. Baublitz, M., Jr. Derivation of the Schrödinger equation from a stochastic theory. *Prog. Theor. Phys.* **1988**, *80*, 232–244. [CrossRef]
6. Anderson, J.B. A random-walk simulation of the Schrödinger equation: H^+_3. *J. Chem. Phys.* **1975**, *63*, 1499–1503. [CrossRef]
7. Laskin, N. *Fractional Quantum Mechanics*; World Scientific Publishing Company: Singapore, 2018.
8. Laskin, N. Fractals and quantum mechanics. *Chaos* **2000**, *10*, 780–790. [CrossRef]
9. Laskin, N. Fractional Schrödinger equation. *Phys. Rev. E* **2002**, *66*, 056108. [CrossRef]
10. Evangelista, L.R.; Lenzi, E.K. *Fractional Diffusion Equations and Anomalous Diffusion*; Cambridge University Press: Cambridge, UK, 2018; p. 395.
11. Herrmann, R. *Fractional Calculus: An Introduction for Physicists*; World Scientific: Singapore, 2011.
12. De Oliveira, E.C.; Costa, F.S.; Vaz, J. The fractional Schrödinger equation for potentials. *J. Math. Phys.* **2010**, *51*, 123517. [CrossRef]
13. Jiang, X.; Qi, H.; Xu, M. Exact solutions of fractional Schrödinger-like equation with a nonlocal term. *J. Math. Phys.* **2011**, *52*, 042105. [CrossRef]
14. Lenzi, E.K.; Ribeiro, H.V.; dos Santos, M.A.F.; Rossato, R.; Mendes, R.S. Time dependent solutions for a fractional Schrödinger equation with delta potentials. *J. Math. Phys.* **2013**, *54*, 082107. [CrossRef]
15. Dong, J.; Xu, M. Some solutions to the space fractional Schrödinger equation using momentum representation method. *J. Math. Phys.* **2007**, *48*, 072105. [CrossRef]
16. Naber, M. Time fractional Schrödinger equation. *J. Math. Phys.* **2004**, *45*, 3339–3352. [CrossRef]
17. Iomin, A. Fractional-time Schrödinger equation: Fractional dynamics on a comb. *Chaos Solitons Fractals* **2011**, *44*, 348–352. [CrossRef]
18. Iomin, A.; Méndez, V.; Horsthemke, W. Comb model: Non-Markovian versus Markovian. *Fractal Fract.* **2019**, *3*, 54. [CrossRef]
19. Petreska, I.; de Castro, A.S.; Sandev, T.; Lenzi, E.K. The time-dependent Schrödinger equation in non-integer dimensions for constrained quantum motion. *Phys. Lett. A* **2020**, *384*, 126866. [CrossRef]
20. Petreska, I.; Sandev, T.; Lenzi, E.K. Comb-like geometric constraints leading to emergence of the time-fractional Schrödinger equation. *Mod. Phys. Lett. A* **2021**, *36*, 2130005. [CrossRef]
21. El-Nabulsi, R.A. A new approach to the schrodinger equation with position-dependent mass and its implications in quantum dots and semiconductors. *J. Phys. Chem. Solids* **2020**, *140*, 109384. [CrossRef]
22. Alhaidari, A. Solution of the Dirac equation with position-dependent mass in the Coulomb field. *Phys. Lett. A* **2004**, *322*, 72–77. [CrossRef]
23. Yu, J.; Dong, S.H. Exactly solvable potentials for the Schrödinger equation with spatially dependent mass. *Phys. Lett. A* **2004**, *325*, 194–198. [CrossRef]
24. Gönül, B.; Özer, O.; GönüL, B.; Üzgün, F. Exact solutions of effective-mass Schrödinger equations. *Mod. Phys. Lett. A* **2002**, *17*, 2453–2465. [CrossRef]
25. Barranco, M.; Pi, M.; Gatica, S.M.; Hernández, E.S.; Navarro, J. Structure and energetics of mixed ^{4}He-^{3}He drops. *Phys. Rev. B* **1997**, *56*, 8997–9003. [CrossRef]
26. Von Roos, O. Position-dependent effective masses in semiconductor theory. *Phys. Rev. B* **1983**, *27*, 7547–7552. [CrossRef]
27. Von Roos, O.; Mavromatis, H. Position-dependent effective masses in semiconductor theory. II. *Phys. Rev. B* **1985**, *31*, 2294–2298. [CrossRef] [PubMed]
28. Sakurai, J.; Napolitano, J. *Modern Quantum Mechanics*, 2nd ed.; Person New International Edition: London, UK, 2014.
29. Ribeiro, H.V.; Tateishi, A.A.; Alves, L.G.; Zola, R.S.; Lenzi, E.K. Investigating the interplay between mechanisms of anomalous diffusion via fractional Brownian walks on a comb-like structure. *New J. Phys.* **2014**, *16*, 093050. [CrossRef]
30. Arkhincheev, V.; Baskin, E. Anomalous diffusion and drift in a comb model of percolation clusters. *Sov. Phys. JETP* **1991**, *73*, 161–300.
31. Wang, Z.; Lin, P.; Wang, E. Modeling multiple anomalous diffusion behaviors on comb-like structures. *Chaos Solitons Fractals* **2021**, *148*, 111009. [CrossRef]
32. Liang, Y.; Wang, S.; Chen, W.; Zhou, Z.; Magin, R.L. A survey of models of ultraslow diffusion in heterogeneous materials. *Appl. Mech. Rev.* **2019**, *71*, 040802. [CrossRef]
33. Bunde, A.; Havlin, S.; Stanley, H.; Trus, B.; Weiss, G. Diffusion in random structures with a topological bias. *Phys. Rev. B* **1986**, *34*, 8129. [CrossRef]
34. O'Shaughnessy, B.; Procaccia, I. Diffusion on fractals. *Phys. Rev. A* **1985**, *32*, 3073–3083. [CrossRef]

35. O'Shaughnessy, B.; Procaccia, I. Analytical Solutions for Diffusion on Fractal Objects. *Phys. Rev. Lett.* **1985**, *54*, 455–458. [CrossRef]
36. Richardson, L.F. Atmospheric diffusion shown on a distance-neighbour graph. *Proc. Math. Phys. Eng. Sci.* **1926**, *110*, 709–737.
37. Boffetta, G.; Sokolov, I.M. Relative Dispersion in Fully Developed Turbulence: The Richardson's Law and Intermittency Corrections. *Phys. Rev. Lett.* **2002**, *88*, 094501. [CrossRef]
38. Daniel ben Avraham, S.H. *Diffusion and Reactions in Fractals and Disordered Systems*; Cambridge University Press: Cambridge, UK, 2000.
39. Su, N.; Sander, G.; Liu, F.; Anh, V.; Barry, D. Similarity solutions for solute transport in fractal porous media using a time- and scale-dependent dispersivity. *Appl. Math. Model.* **2005**, *29*, 852–870. [CrossRef]
40. Shah, K.; Jarad, F.; Abdeljawad, T. Stable numerical results to a class of time-space fractional partial differential equations via spectral method. *J. Adv. Res.* **2020**, *25*, 39–48. [CrossRef]
41. Shah, K.; Naz, H.; Sarwar, M.; Abdeljawad, T. On spectral numerical method for variable-order partial differential equations. *AIMS Math.* **2022**, *7*, 10422–10438. [CrossRef]
42. Khan, H.; Khan, A.; Chen, W.; Shah, K. Stability analysis and a numerical scheme for fractional Klein-Gordon equations. *Math. Methods Appl. Sci.* **2019**, *42*, 723–732. [CrossRef]
43. Bushnaq, S.; Shah, K.; Tahir, S.; Ansari, K.J.; Sarwar, M.; Abdeljawad, T. Computation of numerical solutions to variable order fractional differential equations by using non-orthogonal basis. *AIMS Math.* **2022**, *7*, 10917–10938. [CrossRef]
44. Shah, K.; Arfan, M.; Ullah, A.; Al-Mdallal, Q.; Ansari, K.J.; Abdeljawad, T. Computational study on the dynamics of fractional order differential equations with applications. *Chaos Solitons Fractals* **2022**, *157*, 111955. [CrossRef]
45. Liang, Y.; Chen, W.; Cai, W. *Hausdorff Calculus: Applications to Fractal Systems*; Walter de Gruyter GmbH & Co KG: Berlin, Germany, 2019; Volume 6.
46. Wyld, H.W. *Mathematical Methods for Physics*, 2nd ed.; Advanced Book Classics, Advanced Book Program; Perseus Books: New York, NY, USA, 1999.
47. Mota-Furtado, F.; O'Mahony, P. Eigenfunctions and matrix elements for a class of eigenvalue problems with staggered ladder spectra. *Phys. Rev. A* **2006**, *74*, 044102. [CrossRef]
48. Mota-Furtado, F.; O'Mahony, P. Exact propagator for generalized Ornstein-Uhlenbeck processes. *Phys. Rev. E* **2007**, *75*, 041102. [CrossRef]
49. Bezuglyy, V.; Mehlig, B.; Wilkinson, M.; Nakamura, K.; Arvedson, E. Generalized ornstein-uhlenbeck processes. *J. Math. Phys.* **2006**, *47*, 073301. [CrossRef]